Quantum Transduction of Telecommunications-band Single Photons from a Quantum Dot by Frequency Upconversion

Matthew T. Rakher,[1,*] Lijun Ma,[2,*] Oliver Slattery,[2] Xiao Tang,[2,†] and Kartik Srinivasan[1,‡]

[1]*Center for Nanoscale Science and Technology, National Institute of Standards and Technology, Gaithersburg, MD 20899, USA*

[2]*Information Technology Laboratory, National Institute of Standards and Technology, Gaithersburg, MD 20899, USA*

(Dated: August 17, 2010)

[*]These authors contributed equally to this work.

[†]Electronic address: xiao.tang@nist.gov

[‡]Electronic address: kartik.srinivasan@nist.gov

Transducing non-classical states of light from one wavelength to another is required for integrating disparate quantum systems that take advantage of telecommunications-band photons for optical fiber transmission of quantum information and near-visible, stationary systems for manipulation and storage. In addition, transducing a single-photon source at 1.3 μm to visible wavelengths would be integral to linear optical quantum computation due to near-infrared detection challenges. Recently, transduction at single-photon power levels has been accomplished through frequency upconversion, but it has yet to be demonstrated for a true single-photon source. Here, we transduce triggered single-photons from a semiconductor quantum dot at 1.3 μm to 710 nm with 21 % (75 %) total detection (internal conversion) efficiency. We demonstrate that the upconverted signal maintains the quantum character of the original light, yielding a second-order intensity correlation, $g^{(2)}(\tau)$, that shows the optical field is composed of single photons with $g^{(2)}(0) = 0.165 < 0.5$.

Upconversion is an optical process by which two optical fields combine in a nonlinear medium to generate a third field at a frequency equal to the sum of the two inputs[1]. Along with energy conservation, this process requires momentum conservation, placing a condition on the phase velocities of the three beams. Recently, it has been shown that quasi-phase-matching[2], a process by which a grating in the nonlinear medium is used to compensate for wavevector mismatch between the sum frequency beam and the two input beams, can enable highly efficient upconversion[3], with near unity conversion efficiencies achieved in periodically-poled $LiNbO_3$ waveguides (PPLN WGs). Since upconversion, in principle, can be used to transduce one photon at a given wavelength to a photon at another wavelength, one could imagine using it to couple different quantum systems at different energies[4]. This kind of hybrid quantum information scheme uses photons for efficient transmission of quantum information over large distances[5], and robust, stationary quantum systems such as trapped atoms[6] or ions[7], atomic ensembles[8,9], or spins in quantum dots[10] for manipulation and storage. Another important application of quantum transduction is the frequency upconversion of telecommunications-band photons to the visible part of the spectrum for detection with commercially-available low-noise silicon detectors, for example, as part of a quantum information protocol. The challenges of single photon detection in the near-infrared[11] inhibit the progress of linear optical quantum computation schemes[12,13] because of the stringent requirements on efficient photon detection[14]. That being said, there have been a relatively limited number of upconversion experiments in the quantum domain. In 1992, Huang and Kumar showed[15] that the non-classical intensity correlation between twin

beams at 1064 nm was preserved after one beam was upconverted to 532 nm. In 2001, Kim, Kulik, and Shih used[16] upconversion to implement a complete Bell state measurement in a quantum teleportation scheme. In 2005, Tanzilli *et al.* demonstrated[17] that the time-energy entanglement between two modes at 1555 nm and 1312 nm generated by spontaneous parametric downconversion was maintained after the 1312 nm beam was upconverted to 712.4 nm; similar results have also been recently reported for a different set of wavelengths[18]. While non-classical correlations between the two beams were demonstrated in each case after upconversion, taken individually, each field exhibited classical photon statistics. Recent progress with upconversion detectors has allowed for photodetection at single photon power levels[19–22], although in each case the light detected was a classical source (a highly attenuated laser beam). On the other hand, true (non-classical) single photon generation has been shown to be achievable through excitation of a single epitaxially-grown quantum dot, with experimental demonstrations of stable sources in the 900 nm to 1300 nm region[23–27], but they have not been used for upconversion. Here, we demonstrate for the first time, efficient upconversion of single photons generated by a quantum dot at 1.3 μm to 710 nm. In particular, we measure the second-order intensity correlation of the upconverted 710 nm signal and show that the field is dominantly composed of single photons.

Optical Fiber-based Collection of Quantum Dot Photoluminescence

In our experiments, single photons at 1.3 μm are generated by the recombination of excitons in a single epitaxially-grown InAs quantum dot (QD) embedded in an InGaAs quantum well and within a 256 nm thick GaAs layer. This dot-in-a-well (DWELL) structure enables efficient capture of excitons generated in the quantum well into the QD[28]. Following the work of Ref. 29, QDs are isolated in a mesa (see Methods) where their emission is collected by a fiber taper waveguide (FTW). The FTW is a single-mode optical fiber whose diameter is adiabatically reduced from 125 μm to roughly 1 μm over 10 mm by simultaneously pulling and heating the fiber with a H_2 torch to near the melting temperature of glass[30]. Because the diameter is comparable to the wavelength of light, the field exhibits an evanescent tail of a few hundred nm outside of the physical dimension of the fiber, enabling efficient near-field coupling to nanophotonic devices. As shown in the schematic of Fig. 1a, the QD is optically excited using 50 ps pulses from a 50 MHz laser diode at 780 nm. The laser is sent through a variable optical attenuator and reduced to 10 nW of power (enough to saturate the single exciton QD transition) before being coupled into the FTW. The FTW is incorporated into a liquid Helium cryostat and positioned

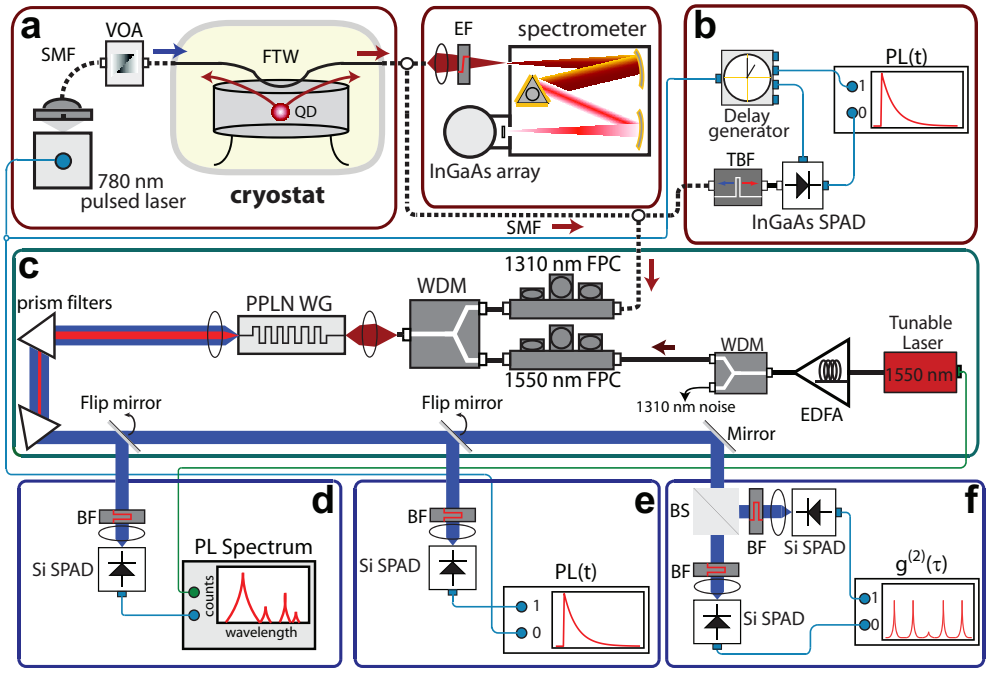

FIG. 1: **Experimental schematic for upconversion of photoluminescence from a QD. a**, Schematic of experimental setup for excitation and collection of QD photoluminescence (PL) by a FTW. **b**, Schematic for time-resolved PL measurement using an InGaAs SPAD. **c**, Upconversion part of experimental setup. **d**, Schematic for PL spectroscopy after upconversion. **e**, Schematic for time-resolved PL measurement after upconversion. **f**, Schematic of Hanbury-Brown and Twiss interferometer after upconversion. Definition of acronyms: PL=photoluminescence, SPAD=single photon counting avalanche photodiode, FTW=fiber taper waveguide, SMF=single mode fiber, VOA=variable optical attenuator, FPC=fiber polarization controller, WDM=wavelength division multiplexer, EDFA= erbium-doped fiber amplifier, TBF=tunable bandpass filter, EF=edgepass filter, BF=bandpass filter, BS=non-polarizing beamsplitter.

into contact with the mesa, which is cooled to about 8 K. The evanescent field of the pump laser mode propagating through the FTW excites carriers into the GaAs where they subsequently optically recombine in the QD, generating photoluminescence (PL). A significant fraction of the photons are emitted back into the FTW and coupled out into the fiber (see Methods). Compared to free-space techniques using a lens or high numerical aperture microscope objective, the FTW probe can theoretically collect up to 10 times more photons[31] and provides a natural interface into single mode fiber for convenient extraction. To measure the QD emission spectrum, we couple the PL into a grating spectrometer with a cooled InGaAs array with ≈ 0.09 nm resolution

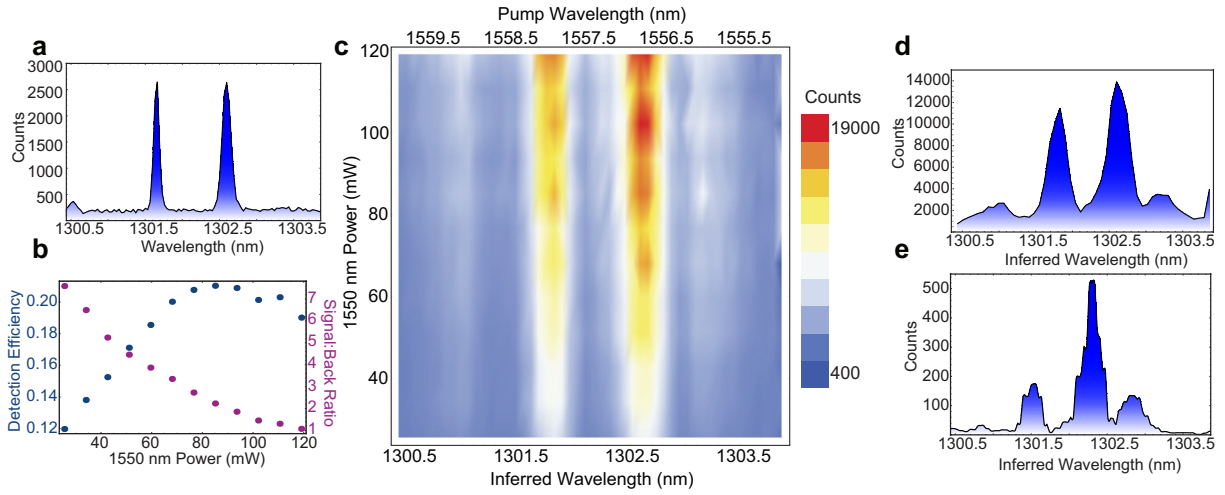

FIG. 2: **PL spectrum of a QD measured by upconversion.** **a**, PL spectrum taken with a grating spectrometer with InGaAs array for 60 s integration time. **b**, Total detection efficiency (blue) and signal count to background count ratio (magenta) for upconversion detection as a function of 1550 nm pump power. **c**, Density plot of the upconverted PL spectrum taken by scanning the 1550 nm pump laser and integrating 1 s at each point as a function of 1550 nm pump laser power. **d**, Single upconverted PL spectrum from **c** with 85 mW of 1550 nm power. **e**, Upconversion response measured by recording spectrum of a laser near 1302.6 nm with 5 MHz linewidth.

as shown in Fig. 1a. Figure 2a shows such a spectrum with 60 s integration time. The sharp lines of a single QD are measured near 1301.6 nm and 1302.6 nm and identified by polarization to be the positively charged and neutral exciton transitions, respectively, of the same QD. Typical measured photon fluxes were 10^4 s^{-1}, corresponding to an average power of 1.5 fW. At these low fluxes, InGaAs detectors are difficult to use because of their high dark count rates and lower gain which necessitate long integration times, usually at least an order of magnitude longer than that required for QDs with emission near 950 nm where Si-based detectors can be used.

Frequency Upconversion Spectroscopy

For comparison, we also measure the PL spectrum using upconversion as shown in Fig. 1c-d following the technique of Ref. 32, 33, and 34. In this experiment, the PL is sent through a fiber polarization controller and combined with a strong optical field near 1550 nm through a wavelength division multiplexer. This field is obtained using a tunable diode laser coupled to an erbium-doped fiber amplifier (EDFA) yielding 25 mW to 120 mW of continuous power into

the PPLN WG. The 1550 nm light is sent through a fiber polarization controller before being combined with the PL and directed into a 5 cm long, temperature-controlled PPLN WG held at 61.0 °C ± 0.1 °C. The strong optical nonlinearity of the PPLN WG enables sum-frequency generation under appropriate quasi-phase-matching conditions (≈ 0.35 nm bandwidth) and creates an optical field near 710 nm where the quantum efficiency of a Si single photon counting avalanche photodiode (SPAD) is ≈70 %. The PPLN WG enables upconversion to 710 nm over a broad wavelength range of 1280 nm to 1340 nm by pump wavelength and temperature adjustment. The light emerging from it is dominantly composed of the upconverted 710 nm signal, the remaining 1550 nm pump, and frequency-doubled pump photons at 775 nm. To remove the 1550 nm and 775 nm light, two dispersive prisms and a 20 nm bandpass filter are employed before detection at a Si SPAD. As shown in Fig. 2b, using a laser attenuated to the same power level as the QD emission, we can determine the total detection efficiency (blue) and signal to background count ratio (magenta) as a function of 1550 nm input power (see Methods). The overall detection efficiency maximum is 21.0 % ± 0.2 % for a pump power of 85 mW, while the signal to dark count ratio is maximized for the minimum power of 25 mW. Taking into account optical losses, a lower bound for the internal conversion efficiency of the PPLN WG with 85 mW of 1550 nm power is estimated to be 75 % ± 1 %. To obtain a spectrum using upconversion, the pump laser was spectrally tuned from 1555 nm to 1559.9 nm in 0.1 nm steps while pulses from the Si SPAD are counted in 1 s bins; in contrast to Fig. 2a, a spectrum is built-up through sequential single-channel measurements similar to that of a scanning monochromator. The resulting spectra as a function of 1550 nm pump power, pump wavelength, and inferred 1300 nm wavelength are shown in Fig. 2c, while Fig. 2d shows a single spectrum taken with 85 mW of 1550 nm pump power. Note the presence of both QD emission lines as in Fig. 2a. The spectrum is limited to a resolution of ≈0.35 nm and contains side peaks because of the sinc^2 transfer function response of the PPLN WG[2], as measured directly in Fig 2e using a narrow linewidth (5 MHz) laser. While this is a limitation of the use of upconversion for high-resolution spectroscopy, of more importance to subsequent photon counting measurements is that a single-pixel signal-to-noise ratio similar to that of Fig. 2a is obtained for 1/60 the integration time.

Time-resolved Photoluminescence

An important counterpart to the aforementioned steady-state spectroscopy is a time-resolved PL measurement which can reveal the excited-state lifetime of the QD transition and provide insight

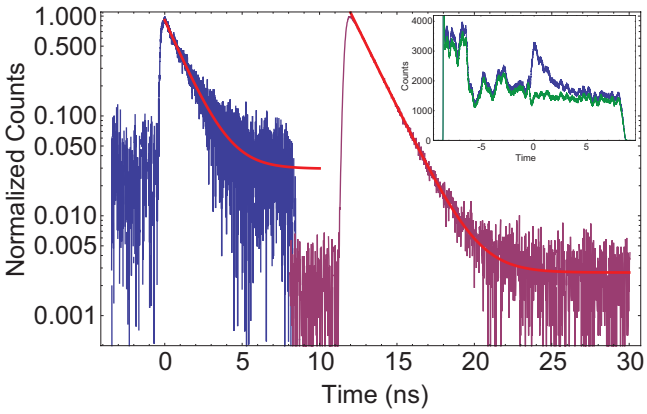

FIG. 3: **Time-resolved PL of a single QD.** PL lifetime measured by the InGaAs SPAD (blue) and the Si SPAD (maroon) after upconversion. Inset: Raw histograms of the signal (blue) and dark-count only (green) traces taken with the InGaAs SPAD.

into effects such as radiative cascades and non-radiative decay. This measurement can be obtained by incorporating a SPAD and a time-correlated single photon-counting (TCSPC) board as shown schematically in Fig. 1b. The TCSPC repeatedly records the time interval between start events triggered by the pulsed laser and stop events triggered by detection of a photon at the SPAD. First, we used a commercial InGaAs SPAD to measure the lifetime of the neutral exciton (1302.6 nm) peak after spectral filtering by a tunable 1 nm bandpass filter. Because of the after-pulsing effects associated with InGaAs SPADs[35], the detector cannot run freely like a Si SPAD and we must run in a gated detection mode as shown in Fig. 1b. Our optimized detection settings were 20 % detection probability, 10 μs dead time, and a 20 ns gate width triggered by a delay generator with delay chosen to match the detection window to the arrival of pulses of PL. Under this configuration, the trigger rate was 4.3 MHz and the measured dark count rate was 12 500 s^{-1}. Because of quantum efficiency oscillations that occur at the start of the gate of our InGaAs detectors, we chose a sufficiently long gate width to avoid these modulations and include the full decay of the PL[26]. The lifetime trace after background subtraction is shown in blue in Fig. 3 for an integration of 700 s. The raw data for the signal (blue) and dark count only (green) measurements are shown in the inset of Fig. 3 where the quantum efficiency oscillations are clearly visible along with the arrival of the optical pulse at 0 ns. Analysis of the background-subtracted trace leads to a measured lifetime (with 95 % confidence interval) of 1.3 ns$\pm$ 0.1 ns and the resulting fit is shown along with the data.

The same lifetime measurement can be performed using a Si SPAD after upconversion as

shown in Fig. 1e. The PL is combined with 25.5 mW of the pump laser at 1556.8 nm in the PPLN WG for efficient upconversion of the neutral exciton transition at 1302.6 nm to 710 nm. Because of the 0.35 nm upconversion bandwidth, no additional spectral filtering is required to select the neutral exciton peak. The freely running SPAD (50 ns dead time, 100 s^{-1} intrinsic dark count rate) provides the stop signal for TCSPC and we integrate for 600 s. To remove background counts, a measurement without the 780 nm excitation is also taken for subsequent subtraction. The resulting measurement in shown in maroon in Fig. 3 and has been temporally offset for comparison with the InGaAs measurement. A fit to the data (red line) yields a lifetime (with 95 % confidence interval) of 1.38 ns$\pm$ 0.03 ns. Figure 3 clearly shows the Si measurement has a dynamic range $\approx$25 times better than that of the InGaAs SPAD and demonstrates the usefulness of upconversion for substantially more sensitive detection.

Second-order Intensity Correlation

To prove that the upconverted 710 nm signal was composed of single photons and inherently non-classical, we measured the second-order intensity correlation $g^{(2)}(\tau) = \langle : I(t)I(t+\tau) : \rangle / \langle I(t) \rangle^2$ using a Hanbury-Brown and Twiss interferometer as depicted in Fig. 1f. After upconversion in the PPLN WG pumped by 85 mW of 1556.8 nm power and spectral dispersion by the prisms, the 710 nm signal was divided by a 50:50 non-polarizing beamsplitter and then directed into two Si SPADs where detection events were used as the start and stop signals for the TCSPC. The histogram of such start-stop events as a function of the time interval is directly related to $g^{(2)}(\tau)$ and is shown in Fig. 4a. The data shows that the areas between PL pulses every 20 ns have a non-zero number of events. Clearly, this time-independent background arises from start-stop events triggered by detection of photons not from the PL of the QD, which decays on a fast timescale ($\tau_{PL} = 1.38$ ns as in Fig. 3) every 20 ns. The origin of these events is the start and/or stop detection of upconverted anti-Stokes Raman (ASR) photons near 1302.6 nm from the pump laser at 1556.8 nm that are transmitted by the 20 nm bandpass filter and compose approximately 1/3 of the total counts (see Fig. 2b). Nonetheless, the peak at $\tau = 0$ is reduced compared to the other peaks by a factor of $0.37 \pm 0.02 < 0.5$, indicating the single photon nature of the light. However, because the ASR photon events are temporally distinguishable from true PL events, this background can be subtracted (see Methods) to obtain the true $g^{(2)}(\tau)$ for the PL signal. In principle, the background can be easily reduced by using smaller bandwidth filters; for instance a 1 nm filter would reduce it by approximately a factor of 20. Another feature of Fig. 4a

is that the peaks nearest $\tau = 0$ at $\tau = \{\pm 20$ ns, ± 40 ns$\}$ do not recover completely even though the QD lifetime is only 1.38 ns. This sub-microsecond correlation effect has been measured previously for QDs[36] and is thought to be caused by the preferential capture of single carriers into the QD rather than electron-hole pairs. The strength of this effect is known to depend strongly on excitation wavelength and power and is not the focus of this work. After background subtraction and normalization by peaks far from $\tau = 0$, $g^{(2)}(\tau)$ can be extracted as shown in Fig. 4b. The reduction at $\tau = 0$ is a clear indication of photon anti-bunching and the non-classical nature of the optical field. The value $g^{(2)}(0)$ can be obtained by comparing counts in the $\tau = 0$ peak to the average of those in the $\tau \neq 0$ peaks and we obtain a value of $g^{(2)}(0) = 0.165 \pm 0.010$. Because $g^{(2)}(0) = 0.165 < 0.5$, the optical field must be dominantly composed of single photons. The measured non-zero value of $g^{(2)}(0) = 0.165$ is due to uncorrelated emission at 1.3 μm collected by the FTW and subsequently upconverted which may be reduced by exciting closer to the QD transition. In addition, the 1550 nm pump power might also be expected to influence the $g^{(2)}(0)$ value and the signal-to-noise given tradeoffs between increased detection efficiency and higher levels of background photons as shown in Fig. 2b. To that end, we performed the $g^{(2)}(\tau)$ measurement at three values of the 1550 nm pump power and the results are displayed in Fig. 4c. The best result (Fig. 4b) was obtained for 85 mW of power which corresponded to the optimum overall detection efficiency (21.0 %) of our setup.

Summary

In conclusion, we have used frequency upconversion in a PPLN WG to efficiently measure single photon PL from a QD emitting near 1.3 μm with Si SPADs. In doing so, we have demonstrated that upconversion can be used for high signal to noise spectrometry and time-correlated photon counting for lifetime measurements. While other groups have shown that superconducting single-photon detectors can be used instead of InGaAs SPADs for such measurements in the near-infrared[37], those detectors are not yet widely available and require cryogenic cooling whereas efficient upconversion can be performed with off-the-shelf components. Additionally, we showed that the quantum mechanical nature of the single-photon stream emitted by the QD at 1.3 μm is successfully transduced over to a 710 nm optical field and in particular we measure $g^{(2)}(0) = 0.165$ for this field. Aside from the clear advantage offered in increased measurement sensitivity, efficient quantum transduction by frequency upconversion has several consequences for quantum information schemes involving stationary quantum systems and photons. Because of the large up-

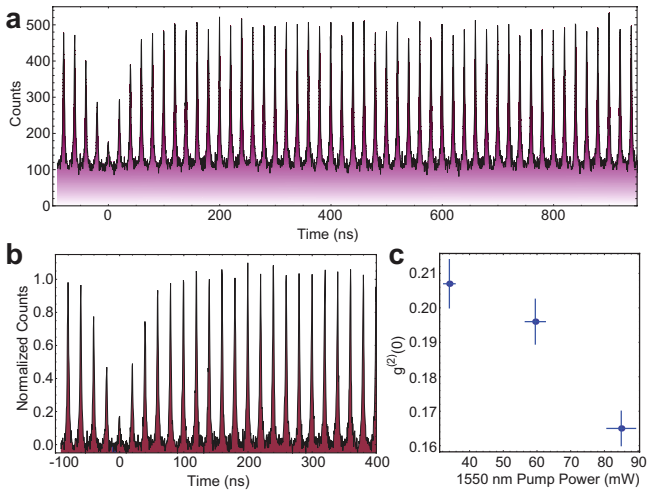

FIG. 4: **Upconversion of single photons.** **a**, Raw histogram of the second-order intensity correlation measurement after 3600 s. **b**, Normalized second-order intensity correlation $g^{(2)}(\tau)$ after ASR photon event subtraction. **c**, $g^{(2)}(0)$ values with errors (see Methods) for different powers of the 1550 nm pump laser.

conversion wavelength range afforded by the quasi-phase-matching of the PPLN WG, QDs with different emission wavelengths as large as several nm (to be expected due to QD growth inhomogeneity) can all be upconverted to the same wavelength. A clear implication of this is that remote operations in the telecommunications-band such as the generation of entanglement[38] between spatially separated electron spins in QDs is possible without the fine spectral-tuning typically required in such schemes. Further, one can envision photon-mediated interactions between electron or hole spins in QDs in the near-infrared with alkali atoms or ions in the near-visible. For example, a hole confined in a QD with an optical transition at 1.3 μm could be coupled to a Rb atom or ensemble[39] at 780 nm by upconversion with a thulium-doped fiber laser at 1.95 μm. Finally, because the upconversion process depends critically on the strong pump field, fast temporal sampling of the input field is possible by using ultrafast pump pulses[40,41]. At present, many time-dependent measurements of QD PL are at best limited to $\approx$40 ps resolution by the Si SPAD timing jitter. Given that pulse widths as short as 4.3 fs have been created using mode-locked fiber lasers[42], QD dynamics on ultrafast timescales could be revealed by upconversion.

Methods

Mesa Fabrication: The QD-containing GaAs layer is isolated 1.5 μm above the rest of the sample surface in a 2 μm diameter mesa. The physical isolation enables efficient probing of a limited number of QDs by the FTW. These mesas are created through: (i) electron beam lithography,

(ii) SF_6/C_4F_8 inductively-coupled plasma reactive ion etching (ICP-RIE) of a deposited Si_xN_y mask layer, (iii) Ar-Cl_2 ICP-RIE etching of the $Al_{0.3}Ga_{0.7}As$ layer and removal of the remaining Si_xN_y layer, and (iv) 20:1 H_2O:HF wet etching of the underlying $Al_{0.7}Ga_{0.3}As$ layer to form the supporting pedestal.

FTW PL collection efficiency: The FTW PL collection efficiency is determined from the measured Si SPAD count rates corrected for the total detection efficiency (21 %) and then normalized to the 50 MHz excitation repetition rate. The normalization is the maximum rate of photon emission by the QD assuming it is excited a single time for each pump pulse. This assumption is valid because the pulse width (50 ps) is much shorter than the radiative lifetime (1.38 ns) and the average power is such that the transition is saturated. For this QD which resides in a non-undercut portion of the mesa, we obtain an efficiency near 0.1 %. This efficiency is consistent with previous experimental work[29] and matches theoretical predictions[31] for a non-undercut dielectric substrate.

Detection and conversion efficiencies: The overall detection efficiency of 21 % is determined with a laser attenuated to a measured power equivalent to the QD (1.5 fW) and set at the wavelength of the neutral exciton transition. The measured Si SPAD count rates after background subtraction are compared to the known input power level. The internal conversion efficiency of 75 % is calculated by correcting the overall efficiency by the measured optical losses ($\eta_{WDM} = 0.95$, incoupling and transmission through the PPLN WG $\eta_{PPLN} = 0.61$, beamsplitter and mirror loss $\eta_{BS} = 0.81$, and $\eta_{BF} = 0.85$) and Si SPAD quantum efficiency at 710 nm ($\eta_{SPAD} = 0.70$). The errors in both efficiencies dominantly result from shot noise in the photon counts. Including the PL collection efficiency, the end-to-end efficiency of the system is ≈ 0.02 %.

$g^{(2)}(\tau)$ background subtraction: As described in the text, background counts are due to ASR photon events and are time-independent. The subtracted level was determined by taking the average number of counts measured for time-delays greater than 8.2 ns from the nearest PL pulse. Since the lifetime was measured to be 1.38 ns, the probability of a PL event contributing at these time delays is negligible (≈ 0.3 %). The background counts observed in the measurement are consistent with what is expected from the ratio of signal to background counts measured in Fig. 2b for 85 mW of pump power. Errors in the extracted $g^{(2)}(0)$ values are determined by the propagation of errors due to shot noise in the $\tau = 0$ peak area, the standard deviation of the peak areas far from

$\tau = 0$, and the shot noise in the subtracted background level.

---

[1] Boyd, G. D. & Kleinman, D. A. Parametric interaction of focused gaussian light beams. *J. Appl. Phys.* **39**, 3597–3639 (1968).

[2] Fejer, M. M., Magel, G. A., Jundt, D. H. & Byer, R. L. Quasi-phase-matched second harmonic generation - Tuning and tolerances. *IEEE J. Quan. Elec.* **28**, 2631–2654 (1992).

[3] Chanvillard, L. *et al.* Soft proton exchange on periodically poled $linbo_3$: A simple waveguide fabrication process for highly efficient nonlinear interactions. *Appl. Phys. Lett.* **76**, 1089–1091 (2000).

[4] Wallquist, M., Hammerer, K., Rabl, P., Lukin, M. & Zoller, P. Hybrid quantum devices and quantum engineering. *Physica Scripta* **2009**, 014001 (2009).

[5] Marcikic, I., de Riedmatten, H., Tittel, W., Zbinden, H. & Gisin, N. Long-distance teleportation of qubits at telecommunication wavelengths. *Nature (London)* **421**, 509–513 (2003).

[6] Boozer, A. D., Boca, A., Miller, R., Northup, T. E. & Kimble, H. J. Reversible State Transfer between Light and a Single Trapped Atom. *Phys. Rev. Lett.* **98**, 193601 (2007).

[7] Olmschenk, S. *et al.* Quantum Teleportation Between Distant Matter Qubits. *Science* **323**, 486–489 (2009). 0907.5240.

[8] Duan, L., Lukin, M. D., Cirac, J. I. & Zoller, P. Long-distance quantum communication with atomic ensembles and linear optics. *Nature (London)* **414**, 413–418 (2001).

[9] Chanelière, T. *et al.* Storage and retrieval of single photons transmitted between remote quantum memories. *Nature (London)* **438**, 833–836 (2005).

[10] Gerardot, B. D. *et al.* Optical pumping of a single hole spin in a quantum dot. *Nature (London)* **451**, 441–444 (2008).

[11] Hadfield, R. H. Single-photon detectors for optical quantum information applications. *Nature Photonics* **3**, 696–705 (2009).

[12] Knill, E., Laflamme, R. & Milburn, G. J. A scheme for efficient quantum computation with linear optics. *Nature* **409**, 46–52 (2001).

[13] Kok, P. *et al.* Linear optical quantum computing with photonic qubits. *Rev. Mod. Phys.* **79**, 135–174 (2007).

[14] Varnava, M., Browne, D. E. & Rudolph, T. How good must single photon sources and detectors be for efficient linear optical quantum computation? *Phys. Rev. Lett.* **100**, 060502 (2008).

[15] Huang, J. M. & Kumar, P. Observation of quantum frequency conversion. *Phys. Rev. Lett.* **68**, 2153–2156 (1992).

[16] Kim, Y.-H., Kulik, S. P. & Shih, Y. Quantum teleportation of a polarization state with a complete bell state measurement. *Phys. Rev. Lett.* **86**, 1370–1373 (2001).

[17] Tanzilli, S. *et al.* A photonic quantum information interface. *Nature* **437**, 116–120 (2005).

[18] Ma, L., Slattery, O., Chang, T. & Tang, X. Non-degenerated sequential time-bin entanglement generation using periodically poled ktp waveguide. *Opt. Express* **17**, 15799–15807 (2009).

[19] Vandevender, A. & Kwiat, P. High efficiency single photon detection via frequency up-conversion. *J. Mod. Opt.* **51**, 1433–1445 (2004).

[20] Langrock, C. *et al.* Highly efficient single-photon detection at communication wavelengths by use of upconversion in reverse-proton-exchanged periodically poled $LiNbO_3$ waveguides. *Opt. Lett.* **30**, 1725–1727 (2005).

[21] Albota, M. & Wong, F. Efficient single-photon counting at 1.55 mu m by means of frequency upconversion. *Opt. Lett.* **29**, 1449–1451 (2004).

[22] Xu, H., Ma, L., Mink, A., Hershman, B. & Tang, X. 1310-nm quantum key distribution system with up-conversion pump wavelength at 1550 nm. *Opt. Express* **15**, 7247–7260 (2007).

[23] Michler, P. *et al.* A Quantum Dot Single-Photon Turnstile Device. *Science* **290**, 2282–2285 (2000).

[24] Pelton, M. *et al.* Efficient source of single photons: a single quantum dot in a micropost microcavity. *Phys. Rev. Lett.* **89**, 233602 (2002).

[25] Strauf, S. *et al.* High-frequency single-photon source with polarization control. *Nature Photonics* **1**, 704–708 (2007).

[26] Zinoni, C. *et al.* Time-resolved and antibunching experiments on single quantum dots at 1300 nm. *Appl. Phys. Lett.* **88**, 131102 (2006).

[27] Shields, A. J. Semiconductor quantum light sources. *Nature Photonics* **1**, 215–223 (2007). 0704.0403.

[28] Stintz, A., Liu, G. T., Li, H., Lester, L. F. & Malloy, K. J. Low-threshold current density 1.3-μm InAs quantum-dot lasers with the dots-in-a-well (DWELL) structure. *IEEE Photonics Tech. Lett.* **12**, 591–593 (2000).

[29] Srinivasan, K., Painter, O., Stintz, A. & Krishna, S. Single quantum dot spectroscopy using a fiber taper waveguide near-field optic. *Appl. Phys. Lett.* **91**, 091102 (2007).

[30] Knight, J. C., Cheung, G., Jacques, F. & Birks, T. A. Phase-matched excitation of whispering-gallery-mode resonances by a fiber taper. *Opt. Lett.* **22**, 1129–1131 (1997).

[31] Davanço, M. & Srinivasan, K. Efficient spectroscopy of single embedded emitters using optical fiber taper waveguides. *Opt. Express* **17**, 10542–10563 (2009).

[32] Ma, L., Slattery, O. & Tang, X. Experimental study of high sensitivity infrared spectrometer with waveguide-based up-conversion detector. *Opt. Express* **17**, 14395–14404 (2009).

[33] Thew, R. T., Zbinden, H. & Gisin, N. Tunable upconversion photon detector. *Appl. Phys. Lett.* **93**, 071104 (2008).

[34] Zhang, Q., Langrock, C., Fejer, M. M. & Yamamoto, Y. Waveguide-based single-pixel up-conversion infrared spectrometer. *Opt. Express* **16**, 19557–19561 (2008).

[35] Ribordy, G. *et al.* Photon counting at telecom wavelengths with commerical InGaAs/InP avalance photodiodes: current performance. *Journal of Modern Optics* **51**, 1381–1398 (2004).

[36] Santori, C. *et al.* Submicrosecond correlations in photoluminescence from InAs quantum dots. *Phys. Rev. B* **69**, 205324 (2004).

[37] Zinoni, C. *et al.* Single-photon experiments at telecommunication wavelengths using nanowire superconducting detectors. *Appl. Phys. Lett.* **91**, 031106 (2007).

[38] Simon, C. *et al.* Quantum communication with quantum dot spins. *Phys. Rev. B* **75**, 081302 (2007).

[39] Eisaman, M. D. *et al.* Electromagnetically induced transparency with tunable single-photon pulses. *Nature (London)* **438**, 837–841 (2005).

[40] Kuzucu, O., Wong, F. N. C., Kurimura, S. & Tovstonog, S. Time-resolved single-photon detection by femtosecond upconversion. *Opt. Lett.* **33**, 2257–2259 (2008).

[41] Shah, J. Ultrafast luminescence spectroscopy using sum frequency generation. *IEEE J. Quan. Elec.* **24**, 276–288 (1988).

[42] Krauss, G. *et al.* Synthesis of a single cycle of light with compact erbium-doped fibre technology. *Nature Photonics* **4**, 33–36 (2009).

Acknowledgements We thank A. Stintz and S. Krishna of the University of New Mexico and O. Painter of the California Institute of Technology for assistance with sample preparation, and M. Davanço of NIST for development of the fiber taper fabrication setup.

Author Contributions M.T.R. and K.S. built the low-temperature measurement setup, L.M., O.S., and X.T. built the upconversion detectors, K.S. fabricated the devices, and M.T.R., L.M., and K.S. performed the measurements. M.T.R. and K.S. wrote the manuscript, all authors contributed to the design of the experiments, and K.S. and X.T. supervised the project.

Author Information The authors declare no competing financial interests. Correspondence and

requests for material should be address to K.S.